The University of Manchester Institute of Science and Technology
PO Box 88, Manchester M60 1QD. Telephone 061-236 3311. Telex 666094

FIELD TESTS AND EXPERIMENTS ON VISIBILITY MODIFICATION

US ARMY
DAJA45-86-C-0001

FINAL REPORT - JULY 1988

2

FIELD TESTS AND EXPERIMENTS
ON VISIBILITY MODIFICATION

US ARMY
DAJA45-86-C-0001

FINAL REPORT - JULY 1988

Department of Pure and Applied Physics

UMIST

Manchester M60 1QD

UK

Prof J Latham
Principal Investigator

Dr M H Smith
Project Coordinator

Dr I E Consterdine
Project Scientist

1. PREAMBLE

For reasons outlined in earlier reports and examined in correspondence with Dr Walter Bach, who made very useful comments, the original goals of this work were not achieved. Although the contract is now terminated we are continuing to explore ideas stimulated by the experiments performed, and are hopeful that at some future time we may achieve the originally specified objectives. Reports on any significant progress will be sent automatically to Dr Bach and to the European Research Office.

Herein, we take the opportunity of gathering together, from the earlier reports, the information currently available, which - as mentioned - we hope will provide a springboard to more useful and specific results.

2. INTRODUCTION

Laboratory experiments on the scavenging of wet aerosol - of controlled sizes ranging from about 0.3 to 50μm - by electrically charged collector drops have been performed by Smith (1976), Barker et al (1983), Barlow and Latham (1983) and others. The consistent result from each of these studies by UMIST scientists was of a pronounced increase in measured values of collection efficiency above those found in the absence of electrical forces.

The study most relevant to the fog-visibility modification issue was that of Smith, who found that water drops of characteristic size around 0.1mm, carrying charges of several tenths of the Rayleigh limit, swept out essentially uncharged water droplets of size within the condensate size-band for fogs, with collection efficiencies E in the range approximately 20 to 25 (the corresponding non-electrical values are significantly less than unity). A crude theoretical model of the capture process provided values of E in reasonable agreement with those measured. This prodigious increase in collection efficiency over the 'classical', non-electrical values, for collector drop sizes and charges which could be produced and utilized in a practical situation, is potentially of great importance with respect to the possibility of modifying fogs in order to enhance the visibility within them. The principal of the technique would be to introduce highly charged drops into a fog. These would scavenge fog droplets with great efficiency - as indicated in the laboratory experiments - and the collector drops (now much larger, having swept out large numbers of fog droplets) would settle from the fog under the influence of gravity, leaving it with a substantially reduced liquid water content - and correspondingly enhanced visibility. Smith found that a unique and crucially impor-

tant feature of this collection process is that the dominant electrostatic effect producing the greatly increased collection efficiency is dipole interaction, rather than coulomb forces, i.e. for the situations of relevance, the attractive force between the large charge Q on the collector drop and the dipole induced by Q in the fog droplet, is much greater than the coulombic attraction between Q and q, the charge on the droplet, which for fogs is generally very small. It follows, to a first approximation, that the collector drop will capture fog droplets - and thus promote an increase in visibility - without discrimination as to the sign and magnitude of the droplet charge q. Thus, the collector drop is not preferentially neutralized as it captures droplets, and its longevity (and efficiency) as a scavenging/modification agent is thereby greatly increased. Dipole forces were also found to dominate capture in the experiments of Barlow and Latham, where the aerosol particles collected were in the approximate size range 0.3 to 3μm; this result offers the possibility of modifying electrically the visibility within particulate clouds of generally smaller size than exist in fogs.

3. COLLECTION EFFICIENCY MODEL

In formulating this model, a similar approach has been taken to the earlier work by Smith, although significant improvements have been incorporated to more closely model the forces acting upon the drop/droplet combination. Throughout this analysis, the fall velocity and trajectory of the larger drop is assumed to be unchanged by the influence of the smaller droplet. Thus, the motions of the droplet may be considered in a co-ordinate frame which remains motionless with respect to the drop.

The forces of greatest significance in drop/droplet interactions under the influence of electrical forces are shown schematically in Fig 1. In the absence of electrical forces, the gravitational forces F_{Rg} and F_{rg}, for the drop and droplet respectively, are exactly counterbalanced by the drag forces F_{Rd} and F_{rd} when the two particles are falling at their terminal velocities. The electrical forces acting on the drop/droplet combination consist of a simple coulomb force, which will generally be insignificant under the circumstances of interest in this study, and an attractive force resulting from the dipole charges induced in the droplet by the much larger drop charge. Thus, employing the notation in the figure, the coulomb force is given by

$$F_C = \frac{Qq}{4 \quad z^2} \qquad (1)$$

The charges induced in the droplet by the drop charge Q may be approximated by a simple dipole consisting of an image charge Q' situated a distance a from the droplet centre and a compensating charge Q" at the centre where

$$Q' = \frac{rQ}{z}, \qquad a = \frac{r^2}{z}, \qquad Q" = -Q'$$

The attractive force between the drop and droplet due to this dipole is give by

$$F_D = \frac{Q^2 r}{4 \quad z} \quad \frac{1}{(z - a)^2} - \frac{1}{z^2} \tag{2}$$

which reduces to

$$F_D = \frac{Q^2 rz}{4} \quad \frac{1}{(z^2 - r^2)^2} \quad \frac{1}{z^4} \tag{3}$$

At large separations ($z>3r$), this equation agrees with more precise solutions which take multiple images into account, such as that of Davis (1964). However, for smaller separations, Eq. 3 increasingly underestimates the attractive force and a method of more accurately calculating this force was investigated.

Comparisons of the dipole forces calculated by Davis with values derived from the above expression, under similar circumstance, suggested that a closer approximation F'_D to the multiple image solution could be achieved, without significantly increasing the computational effort by adjusting the result of Eq. 3 by means of the simple regression equation

$$F'_D = F_D \exp(m.\log_e(p) + c) \tag{4}$$

where $p=1/(z/(R+r)-1)$, $m=0.6649$ and $c=-1.2021$. Eq. 4 provides values which agree to within a few percent with the examples given by Davis, for $6 < p < 600$, i.e. for separations of from about 10 to 0.1μm for typical drop/droplet combinations.

It is clear that the smaller droplet must experience non-Stokesian drag forces, if it is to be captured by the charged drop. In the extreme case, a droplet, captured after following the limiting trajectory about the drop, must acquire a velocity

substantially greater than its normal terminal velocity and in excess of the terminal velocity of the larger drop. Therefore, a polynomial approximation formula, valid for Reynolds numbers R_e in the range $0.02 < R_e < 350$, was utilized to relate the droplet velocity to the forces upon it, Pruppacher and Klett (1978). This expression is as follows

$$Y = B_0 + B_1 X + \ldots\ldots + B_6 X^6 \qquad (5)$$

where $X = \log_e 8 \, \frac{{}_a F_d}{{}^{2}_{a}}$, $R_e = \exp(Y)$ and

$B_0 = -0.318657 \times 10^{1}$ $\quad$ $B_1 = +0.992696$

$B_2 = -0.153193 \times 10^{-2}$ $\quad$ $B_3 = -0.987059 \times 10^{-3}$

$B_4 = -0.578878 \times 10^{-3}$ $\quad$ $B_5 = +0.855176 \times 10^{-4}$

$B_6 = -0.327815 \times 10^{-5}$

The model is initialized with the droplet at a substantial distance from the drop and with both particles falling at their terminal velocities. The forces acting upon the droplet are calculated, with the drag force being derived by Newton's method utilizing Eq. 5, and resolved into their X and Y components. Any incremental change F in the algebraic sum of these forces must be employed in overcoming both the droplet inertia and the drag forces acting upon it. Thus, the change in droplet velocity U which occurs within a time step t is related to F by

$$F = \frac{U \; F_{drag}}{U} + \frac{m}{t} \qquad (6)$$

where m is the droplet mass.

Utilizing these equations, trajectories of droplets approaching a given drop may be calculated numerically for a variety of initial conditions and the critical trajectory for which the droplet is just captured by the drop established. The collection efficiency E for a specific drop/droplet combination

is then derived from

$$E = \frac{X_c^2}{(R+r)^2} \tag{7}$$

where X_c is the initial displacement along the X axis for this critical trajectory.

It may be noted that no account is taken in the model of the repulsive forces resulting from the compression of the air film between the drop and droplet. Since these forces are only significant at very small separations between the two particles, they can only serve to slightly delay their inevitable coalescence in situations where the droplet has been attracted to the drop from much greater distances.

Examples of droplet trajectories computed by this model are shown in Figs 2 and 3 and illustrate the paths taken by droplets with differing starting positions. The dots on these figures mark successive droplet positions after each time step (50μs in these cases) and demonstrate the accelerations encountered by the smaller particle as it is drawn toward the drop by the dipole force. In Fig 2, the charge on the 40μm radius drop is almost equal to its Rayleigh limit charge and consequently the collection efficiency is more than 30, compared with a value of less than 0.5 in the absence of electrical forces. Whilst the hydrodynamic collection efficiency is only slightly higher for the 70μm drop shown in Fig 3, its electrical equivalent is much reduced compared with the previous case - despite the similar value of the electric charge - due to the reduced interaction time resulting from the greater relative velocity of the two particles.

Values of collection efficiency E, derived in a similar manner, for a range of drop and droplet sizes and charges are presented in Table 1, where they may be compared with hydrodynamic collection efficiencies estimated from Hocking and Jonas (1970). It may be noted that, for the high values of electrical charge considered in these studies, E is approximately proportional to the drop charge Q, which serves to emphasize the importance of maximizing the drop charges disseminated in the proposed field experiments. Also, E is not a sensitive function of the droplet radius r, showing a slight decrease as r is reduced which is probably a consequence of the increased relative velocity. However, as seen from the table, the 'gain' in E is very dependent upon r since the collection efficiency, in the absence of electrical forces, is a very strong function of r for values of $r/R \lesssim 0.2$. As mentioned previously, E is reduced as R increases due to the higher drop-droplet relative velocity. Thus, to optimize the fog clearing effect, the drops should be as small as is feasible, commensurate with their being large enough to settle to the ground within the requisite time-scale.

TABLE 1

25% Rayleigh Charge				50% Rayleigh Charge	
Drop Radius (μm)	Droplet Radius (μm)	Collection Efficiency	Gain	Collection Efficiency	Gain
60	10	3.49	7	8.0	14
60	5	4.1	30	7.9	59
50	10	5.7	11	11.1	22
50	5	5.6	48	10.6	90
40	10	8.5	19	16.4	36
40	5	8.3	83	15.3	153
30	10	14.3	84	27.0	159
30	5	13.2	1015	23.8	1831

As mentioned in the Introduction, if the capture of the droplets relied upon coulomb forces, the effect of the high drop charge might be quickly neutralized thereby limiting the effectiveness of this technique. However, the role of the dipole forces is such that the drop may grow to a substantial degree whilst still maintaining an enhanced capture efficiency. This point is illustrated in Table 2 which contains values of E calculated assuming that the drop maintains the same electrical charge but increases in size as it passes through a cloud of droplets. It may be noted from this table that, after growing from 30 to 70μm in radius - representing an approximately 13-fold increase in volume - the drop still retains a collection efficiency considerably in excess of its hydrodynamic counterpart. For this idealized case of a fog with a liquid water content of 0.2 $g.m^{-3}$ and containing monodisperse droplets of 5μm radius, the drop would have collected a total of almost 4000 droplets and fallen a distance of about 140m in achieving this growth.

TABLE 2

PERSISTENCE OF ELECTRICAL EFFECT

$r = 5\ \mu m$, $Q = 1.672 pC$ (50% Rayleigh limit at 30 μm)

Drop Radius (μm)	Electrical Collection Efficiency	Hydrodynamic Collection Efficiency	Gain
30	23.8	0.013	1831
35	15.3	0.057	271
40	10.4	0.10	104
45	7.3	0.11	66
50	5.3	0.12	44
55	3.9	0.13	31
60	3.0	0.14	22
65	2.3	0.15	14
70	1.9	0.2	9
80	1.4	0.27	5

4. FOG DISPERSAL MODEL

Using the previously calculated collection efficiencies for charged drops, a simple model was developed to study their effect on a uniform cloud of smaller droplets. The charged drops were injected into the cloud at a height of 4m above the ground and were assumed to reach their terminal velocities instantaneously. The cloud was assumed to consist of droplets of diameter 8μm at a concentration of 200/ml - a typical value for a site near the base of a cap-cloud at Great Dun Fell. The model program ran iteratively, recalculating drop diameters, collection efficiencies and fall rates after each 1mm vertical path had been covered by the drops. A sample output from the model (Figure 4) shows the behaviour for droplets charged to 25% of their Rayleigh limit and having three different initial diameters. The clearance in the first millimetre of fall was chosen to be 10% (by concentration) such that the "release rate" parameter could be calculated for each drop size. We can see from the plot (Figure 4) that there are several advantages in having the injected drops as small as possible. Firstly, the overall clearance is greatest because the smallest drops have the largest increase in collection efficiency over uncharged drops and also have the largest absolute collection efficiency. Secondly, the path length over which the cloud is affected is the longest because the smallest drops have the lowest fall speeds and even though they collect more droplets and more than double in size as they fall, their final size is still less than the drops in the other two groups. Thirdly, the release rate for this size group is the smallest; primarily because the number of collectors is a maximum for the smallest drops, but also because of their increased collection

efficiency which means that only a slightly increased number of collectors is required compared with the other two size groups.

5. PLANS FORMULATED FOR THE FIELD EXPERIMENTS

A field trial will take place in June 1986 about halfway up Great Dun Fell at Greencastle (Map ref. 715310). Greencastle is a steep sided valley which faces S.W. and therefore any westerly wind tends to be channelled up the valley. The release site will be at the entrance to the valley and measurements will be taken of cloud droplet spectra, windspeed and wind direction, temperatures and electric field strength some distance (~150 m) up the valley (downwind of the site).

Water is to be injected continuously into the cloud in the form of droplets sprayed from seven nozzles along a length of pipe, each nozzle about 1 metre from its neighbours and 4 metres above the ground. The sprayed droplets will have initial diameters in the range $60 \leq d_i \leq 100$ µm and, when charged will have 25% of their Rayleigh limit charge upon them. For these test purposes, single sign charging may be employed because the proximity to the ground precludes the build-up of a large space charge. Under operational circumstances, alternate bands of oppositely charged droplets would be utilized to reduce the overall electric field and minimise the onset of corona discharges which would tend to discharge the electrified droplets. The droplets will be charged periodically and the period will be determined by the prevailing windspeed i.e. we require the charge on and off periods to match the time taken for the cloud to travel from the release to the measurement site. The charging is achieved by an inverter multi-stage Cockcroft-Walton voltage doubler circuit powered by a 12V heavy duty battery, the output from which is fed to the insulated water storage tank. The storage tank does not have to be large for the purposes of these experiments as it may be refilled during the periods when the high voltage is not

applied to the spray system. Figure 5 is a schematic diagram of the release site and figure 6 shows the H.T./Refill pump control circuit.

6. PLANS FORMULATED FOR THE DATA ANALYSIS

The experiment has been designed such that the effect we seek will be of a periodic nature; droplets are injected continuously into the cloud but they are charged only periodically. Therefore, a Fourier analysis on the data should produce spectral peaks corresponding to the frequency of the charge/no charge cycle. The FSSP will sample the cloud at a rate of 10Hz which implies an upper limit of 5Hz for meaningful output data from the fast Fourier transform. The lower limit for meaningful data is dependent upon the number of points taken in the set to be transformed. If we take 4096 points then this gives a lower frequency limit of $5/4096 \simeq 1/819$ Hz or a period of about 15 minutes. Therefore, in order that we have significant statistics i.e. more than just one transform, we should expect the experiment to run for extended periods of the order of a few hours or so.

A further route for the analysis is the use of the fast Walsh transform. In this type of analysis the output spectrum yields details of any square-wave components in the input data set rather than the sine waves of the Fourier technique. Since we are in fact using a square wave of charge on/charge off this route may prove more productive and will be investigated further in the near future. All the above arguments about the data set refer equally well to the Walsh analysis.

7. FIELD EXPERIMENTS

This section concerns the findings of a set of field experiments carried out below the summit of Great Dun Fell (GDF) in a steep-sided south-west facing valley (Greencastle). The reasons for choosing this site include the fact that most winds, with a westerly component to their direction, tend to be channelled by the valley sides such that any injected plume has a greater chance of passing through a distant measurement site than in previous experiments sited at the mountain summit.

Prior to any full data collecting runs, and in the absence of any cloud, it was possible to monitor the plume of the injected charged drops. This was achieved using UMIST-built electric field sensors which consisted of weak beta-decay radioactive sources situated 1 metre above, but electrically connected to, the input of a high input impedance voltage follower circuit. With two of these devices, it was possible to determine that the injected plume was some 15 metres wide at an approximate range of 30 metres downwind of its release.

Data were collected from two runs on two separate days. The first was on the morning of the 11 June and the second took place towards the end of 12 June. Due to the constant failure of the automatic control system at the release site, both runs had to be completed with manual control over the release of the charged drops. The period of the charge on/off cycle in both cases was 20 seconds.

The data which was thus collected is presented as sample cloud spectra and as power spectral density (P.S.D.) plots derived from Fast Fourier Transforms on consecutive data points. The PSDs show no significant peaks around the frequency $f =$ 0.005 Hz, which corresponds to our release period, and we must

conclude that we have not significantly altered the composition of the droplet spectra in either of the two cases.

(a) CASE I - 11 June 1986

The surface synoptic chart for 0600 GMT had a shallow and filling depression, centred over the Shetland Islands, and a building ridge of high pressure extending from S.E. Iceland, over Ireland and down to the continent via Wales and S.W. England. In the region of GDF, the surface winds were light and from the north-west. In Greencastle, however, the channelling by the valley sides held the wind direction to about 220°. The associated cloud cover in Greencastle was a thin cap-cloud whose base was approximately 100 metres below the release site. At the measurement site, another 50 metres or so higher, the cloud liquid water content L was recorded at 0609 hrs to be 0.05 gm^{-3}. Figure 7 shows the 1 minute average droplet spectrum around this time. We can see from the figure that the cloud was quite thin with less than 100 drops cm^{-3}, centred around a peak at 8μm diameter. This cloud was also very variable; Figure 8 shows the one-minute averaged droplet spectrum around 0611 hrs merely two minutes after Figure 7. We can see that this spectrum contains double the droplets and, when integrated, yields almost triple the water content as that of Figure 7. This natural variability continued throughout the period of the run (0600-0710 hrs). The most probable cause is that cloudbase was lifting throughout the period and the site was well within the region of near-cloudbase humidity fluctuations which have been shown by Choularton et al (1986) to influence droplet spectra. Figures 9 and 10 show the droplet spectra in the middle and towards the end of the run respectively. When cloudbase had finally lifted clear of the site it became possible to ascertain that there was no other cloud cover in the vicinity.

With the above in mind, we proceeded with the Fourier analysis of the data. The droplet spectra were recorded at a rate of 5 per second (data rate = 5 Hz) which gives a maximum frequency for meaningful output of the Fourier transform fmax = 2.5 Hz, this is called the Nyquist or folding frequency (Otnes and Enochson, 1956) above which aliasing will occur in the transform. The minimum frequency is determined by total record length and represents the frequency of one complete sine cycle throughout the data set. Using these boundaries, Figures 11 and 12 were produced which represent the power spectral density function of our input (droplet concentration) record. The frequency of our charge/no charge cycle was chosen to be 0.05 Hz and if we look on Figure 11 we do, indeed, see a large peak in the PSD. At first, this appeared to demonstrate the effect of charge injection; however, this plot is for the data from the first half hour or so of the run, whilst Figure 12 is for the next 40 minutes of the run, and here, at 0.05 Hz, we see exactly the opposite, ie. a trough in the PSD. It seems that natural variability has swamped out our input (charge) waveform.

(b) CASE II - 12 June 1986

By mid-day on the 12th, the region of high pressure had moved steadily S.E., to become centred over Kent, and it continued to move slowly S.E. until midnight. A surface warm front passed through the GDF area around midday moving N.E., and the associated cold front was in the vicinity of GDF by midnight. In Greencastle, throughout the experimental period, the wind direction was 240°. Light showers were observed between 2000 GMT and the end of the run. The run lasted from 2100 to 2230 GMT. Local cloudbase moved inexorably down the fell, at 1800 GMT it passed

through the summit of GDF and at about 2100 GMT it passed through the measurement site - Figure 13 shows the one-minute averaged specrum around this time - it shows a large number >400 cm^{-3} of small droplets d < 6 μm yielding a low liquid water content L = 0.05 gm^{-3}, all of which are typical of the region around cloud-base of a GDF cap cloud. Cloudbase continued to fall throughout the run and the cloud consequently thickened. By 2141 (Figure 14) L was 0.25 gm^{-3} made up from a spectrum still containing more than 400 drops cm^{-3} but now with a mean diameter d ~ 8 μm. Towards the end of the run at 2115 (Figure 15) the spectrum was very similar but with a slight drop in concentration to about 360 cm^{-3}, and a slight broadening of the spectrum. Figures 16 and 17 are representative outputs from the Fourier analysis. Both figures again indicate a peak which is no larger than others in the spectrum. Figure 17 does look more promising - it is an average of a much larger data-set, and the peak around 0.05 Hz, although broad, is certainly the highest in the spectrum.

Obviously, more work can be done with this data - such as to see if any spectral changes can be identified between periods of charge and periods of no charge - but the Fourier analysis would suggest that these changes may be there but on average will be small.

8. DISCUSSION OF THE FIELD EXPERIMENTS

The lack of any discernible changes in the properties of the clouds at Great Dun Fell due to the injection of charged drops could be due to two problems: firstly, the clouds encountered during the test period exhibited pronounced natural variability which made it extremely difficult to observe any effects. Secondly, estimates of the injected drop charges suggests that they were about 10 to 20% of the Rayleigh limit charge and may have been even lower than these values in the damp cloudy environment of the field experiments. Such values of electric charge should still significantly increase the drop collection efficiencies over their uncharged hydrodynamic values but would limit, to a substantial extent, their effectiveness in the field trials.

In order to overcome these problems, and to demonstrate clearly that electrical forces can be utilized to modify drop collection efficiencies, a new approach is being attempted during the forthcoming Spring field studies.

In these investigations, it is proposed to inject extremely highly charged drops into a natural cloud and to measure, directly, their growth due to the collection of cloud droplets. The charged drops will be produced by a process demonstrated by Vonnegut & Neubauer (1952) in which water drops are ejected from the tip of a capillary needle raised to a high electric potential. By judicious choice of voltage, water pressure and capillary radius, almost monodisperse drops carrying up to about 80% of their limiting charge ay be produced with sizes from about 40 to 200 μm. It is proposed to measure the change in dimensions of these drops as they pass through varying heights of cloud util-

ising our PMS Optical Array probe.

Whilst this technique is not readily adapted to producing the large numbers of injected drops required by a large-scale experiment, it should prove appropriate for the demonstration of the technique, after which the engineering problems associated with the dispersal of numerous highly charged drops could be more optimistically explored.

9. NOTE ON THE GENERAL PHILOSOPHY FOR THE FIRST EXPERIMENT

The experiment was an attempt to monitor changes in cloud droplet number concentration due to the injection of charged drops. Due to the natural variability of the clouds which typically are encountered at GDF it was envisaged that we would inject drops continuously and charge them periodically. The drops injected were of the order of 100μm in diameter and during their fall time, even though the theory suggests that they would sweep out a significantly greater fraction of the smaller cloud droplets when charged than when uncharged, they themselves would not drastically change in diameter. The probe used to sample the cloud, a PMS FSSP, is not capable of sizing the injected drops as they are too large and so the result of cyclic charging should be a corresponding cycle in the number concentrations of the cloud drops as measured at the probe. Although the period of the charge/no-charge event was stated to be 20 seconds (i.e. 10 seconds of charge and 10 seconds of no charge), there are non-zero rise and fall times for the charging system which tend to round-off the edges of the transitions. This makes the input cycle less like a square-wave and so we decided to employ Fourier rather than Walsh analysis techniques.

The input time series to the Fast Fourier Transform algorithm was the 0.2 second integrated cloud droplet number concentration as recorded by the FSSP.

The sampling period used in the analysis is indeed merely a quarter of that envisaged in the original plan. This was because of the brevity of the cloud occurrences during the experiment. In an attempt to gain better statistics i.e. more transforms per data run, it was decided to reduce the number of samples to 1024. It is entirely feasible for the authors to incorporate range-bars

in the plotted data.

10. SPRING 1987 FOG DISPERSAL STUDY

As noted in the 2nd Interim report, the inconclusive results from the earlier field project led to a new approach being attempted during the Spring 1987 field studies.

The basis of this approach was to inject extremely highly charged drops into a natural cloud and to measure, directly, their growth due to the collection of cloud droplets. The work of Smith (1975) indicated that drops of around 80 to 100μm radius, charged to about 80% of their Rayleigh-limit maximum charge would possess collection efficiencies approximately 20 times greater than their geometric sweep-out volumes. Thus, for example, a drop of radius, R, would sweep-out, in falling a distance, l, through a cloud, a volume, V, given by the expression:

$$V = E\,l\,(R+r)^2 \qquad (1)$$

where r is the assumed cloud droplet radius and E is the collection efficiency for the drop.

If we assume, for the sake of simplicity, that the cloud of liquid water content, W, consists of monodisperse droplets of radius, r, then the droplet concentration, N, in the cloud is given by:

$$N = \frac{3\,W}{4\quad r^3} \qquad (2)$$

Therefore, the drop, in passing through the cloud, will collect a total of n droplets where

$$n = V\,N \qquad (3)$$

and the new drop radius, R', will be given by the expression:

$$R' = R^3 + n\,r^{3\;1/3} \qquad (4)$$

Substituting in expressions (1) to (4) for a drop of radius 80µm with a collection efficiency of 25 and a fall path of 3m through a cloud of liquid water content of 0.5 gm^{-1}, we obtain a change in drop radius of about 10µm. A change of this magnitude should be detectable with an optical array probe (OAP), provided that the drop generator is capable of producing monodisperse particles.

11. EXPERIMENTAL ARRANGEMENT UTILISED IN SPRING 1987

An electrostatic droplet generator (Vonnegut & Neubauer, 1952), very similar to that employed in the earlier work by Smith, was constructed to ensure that very highly charged mono-disperse droplets were produced. This device, shown schematically in Fig 1, was adapted for use in cloud by fitting a ventilation hose so that dry air could be supplied to the generator, in order to prevent moisture from causing excessive current leakage from the high voltage (around 15kV) supply. This device worked very well in the laboratory, providing a steady steam of highly charged drops at rates of a 100 to 200 per second.

For operation in the field, this device was mounted on a 'cherry picker' so that the generator could be moved in various directions in order to help in targetting the collector drops on to the OAP. Thus, the drop generator could be aligned just above the OAP, to permit checking of its functioning and the drop size distribution, before moving it to a new position several metres above and upwind of the OAP for the measurements of drop growth. The data gathering computers could be set up to provide fast on-line displays of drop spectra to assist in the targetting of the highly charged drops.

The equipment was set up in the manner outlined above during Spring 1987 and all the systems worked satisfactorily. However, it proved impossible to direct the drops into the sensitive volume of the OAP sizing instrument during the experiment. Basically, the drop stream could be observed quite clearly and targetted into the vicinity of the OAP but the drops proved to be too highly charged to pass unhindered through the sampling volume, being deflected to some part of the grounded casing of the instrument in all circumstances.

12. CONCLUSIONS FROM THE SPRING 1987 EXPERIMENTS

Despite various attempts to demonstrate the feasibility of modifying the structure of clouds and fogs by the injection of highly charged particles, the results have been inconclusive. In both field cases, it is felt that the experiments have been defeated by the engineering requirements of a suitable drop producer, as has probably been the case in several other field trials of electrical fog modification, for example, Loveland et al (1972) and Clark et al (1973). Indeed, the development of a suitable charged drop generation system is probably the key factor in the successful application of the laboratory results to natural fog conditions. Accordingly, considerable further thought has been applied to this problem, as outlined below.

13. THE FUTURE DROP GENERATOR DEVELOPMENT

To maximize the efficiency of the injected charged drops, they need to be reasonably monodisperse and, ideally, with radii around 30 to 50μm, with charges as close as possible to the Rayleigh limit. Since, in an operational project, the drops must be produced in substantial quantities, the resultant high space charge tends to result in opposing forces which inhibit the generation process, as noted in Smith (1972). Thus, extremely severe requirements are placed upon the generation system. These requirements may be ameliorated, in principle, in a full-scale system by producing drop populations of <u>both</u> signs, but will need to be taken into account in the design of the individual charged drop generators.

Firstly, considering the problems of charging the particles, we may note from the earlier studies that techniques relying on induction charging mechanisms where, typically, a high voltage electrode is placed near the region of drop production, result in particle charges of up to about 20% of the Rayleigh limit. Applying high electrical potentials directly to the fluid can provide much larger drop charges which approach more closely the Rayleigh limit, i.e. up to 80% or more, with the added attraction that the electrostatic forces can assist the atomization process (or, indeed, drive it as in the case of the Vonnegut & Neubauer generator).

One means of producing substantial numbers of monodisperse drops utilizes an air-driven spinning top, as described in May (1966). This technique can be scaled up by employing a larger spinning disk which is able to cope with the quantities of liquid required and forms the basis of some electrostatic paint-spraying techniques. However, the need for relatively small, monodisperse

drops places severe requirements on the motor and bearings of a practical system. Also, the necessity of applying high electrical potentials to the rotating disk both to charge the drops and assist with the atomization process means that the motor must be capable of a high degree of electrical isolation. Air-driven motors are now fairly readily available and are frequently used in high-speed drilling and sanding equipment. Thus, it is suggested that a motor of this type, fitted with a well-machined disk could form the basis of a suitable drop generation and charging system. Work on a dispensing system employing this approach has already been started at UMIST.

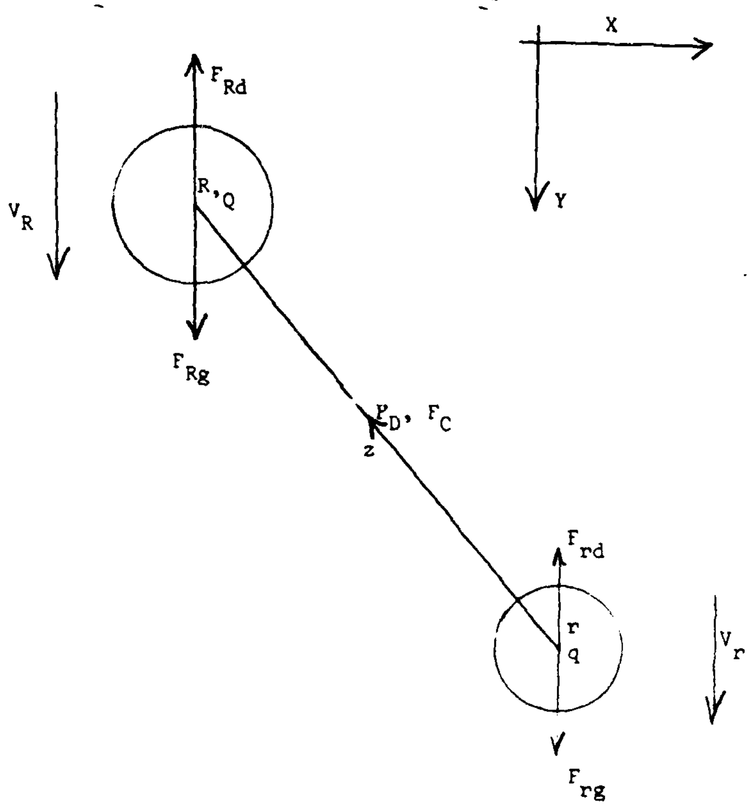

Schematic diagram of drop/droplet interaction

Fig 1

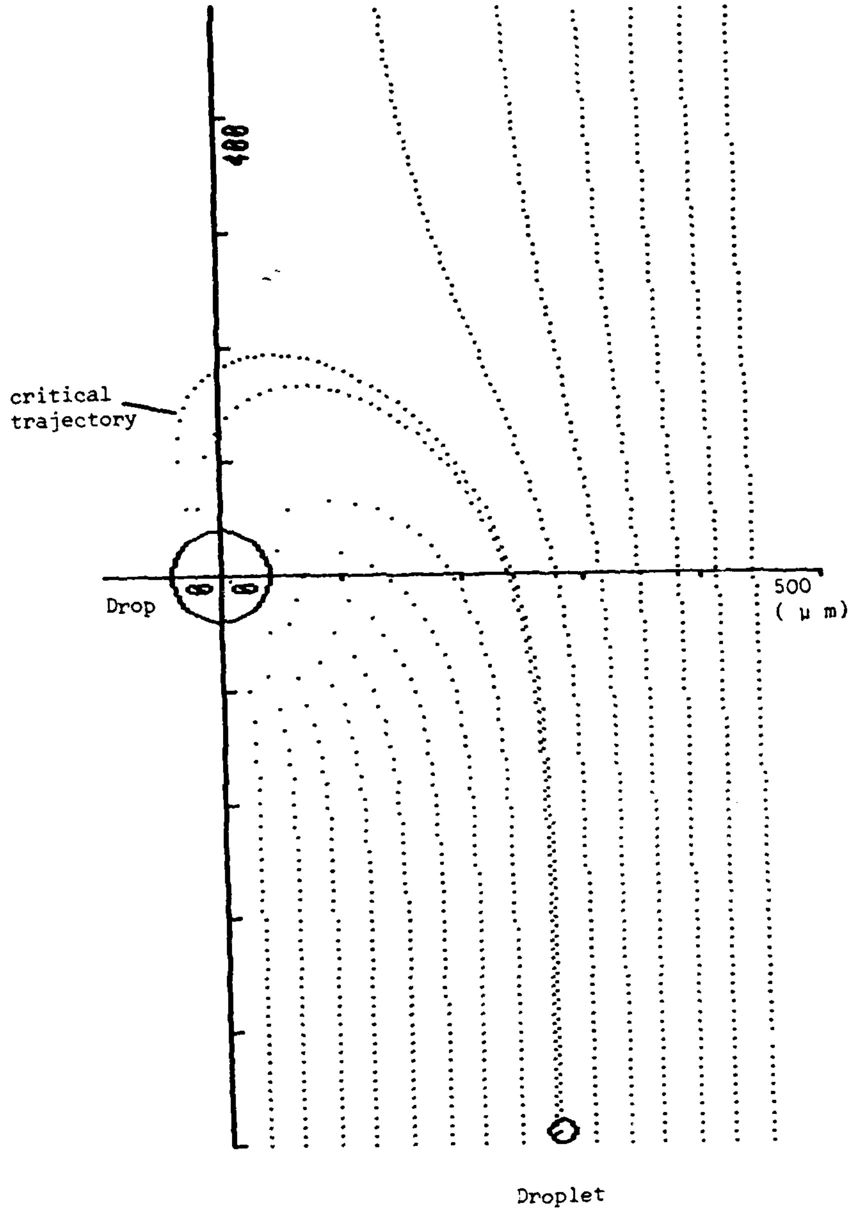

Drop and droplet radii :   4Ø 1Ø
Drop Charge :   5.ØØØ pC
Rayleigh Limit Charge :   5.15Ø pC
% Rayleigh Charge   :   97.Ø9
Droplet Charge :   Ø.ØØØ fC
Drop Velocity   :   Ø.175 m/s
Droplet Velocity :   Ø.Ø14 m/s
Collection Efficiency :   3Ø.47

Fig 2.

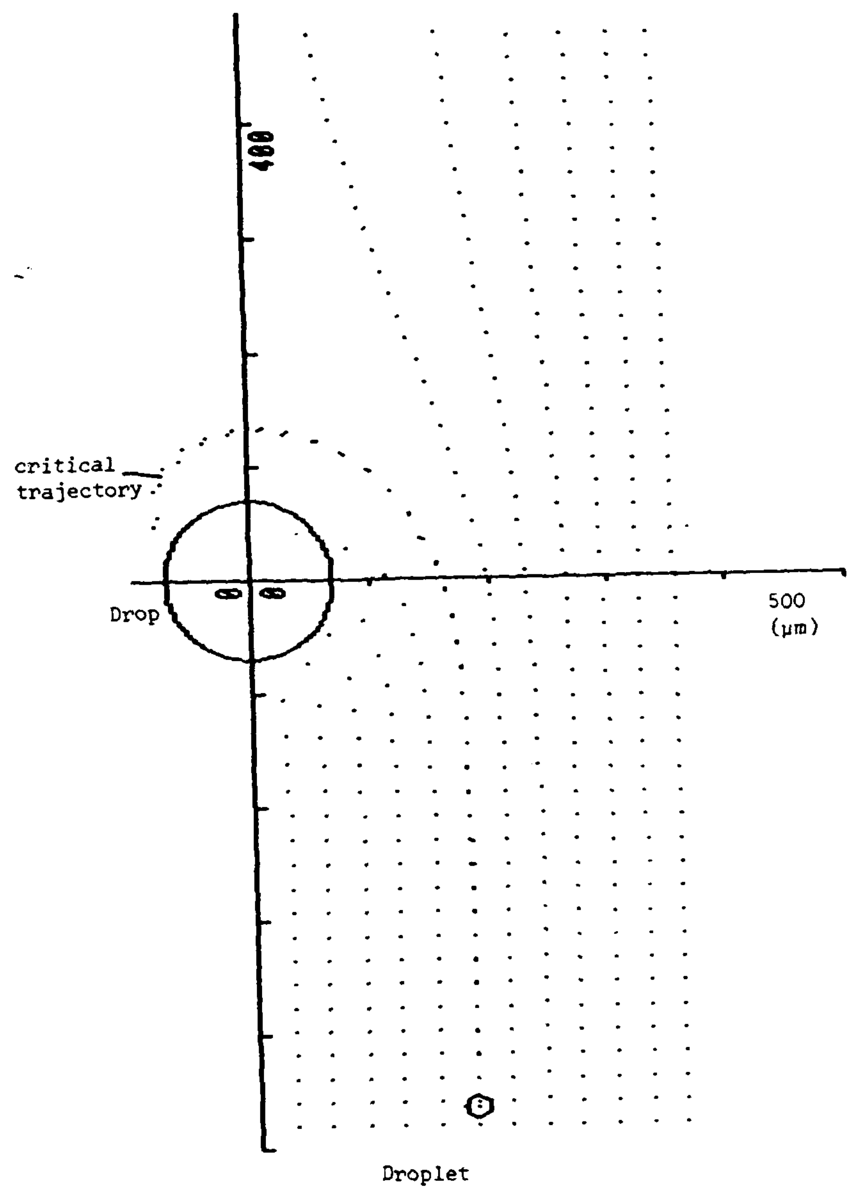

Drop and droplet radii : 70 10
Drop Charge : 5.000 pC
Rayleigh Limit Charge : 11.922 pC
% Rayleigh Charge : 41.94
Droplet Charge : 0.000 fC
Drop Velocity : 0.429 m/s
Droplet Velocity : 0.014 m/s
Collection Efficiency : 5.18

Fig 3.

Cloud droplet diameter = 8 microns
Windspeed = 10 m/s
Fraction of Q(Rayleigh) = 0.25
Release height = 4 m

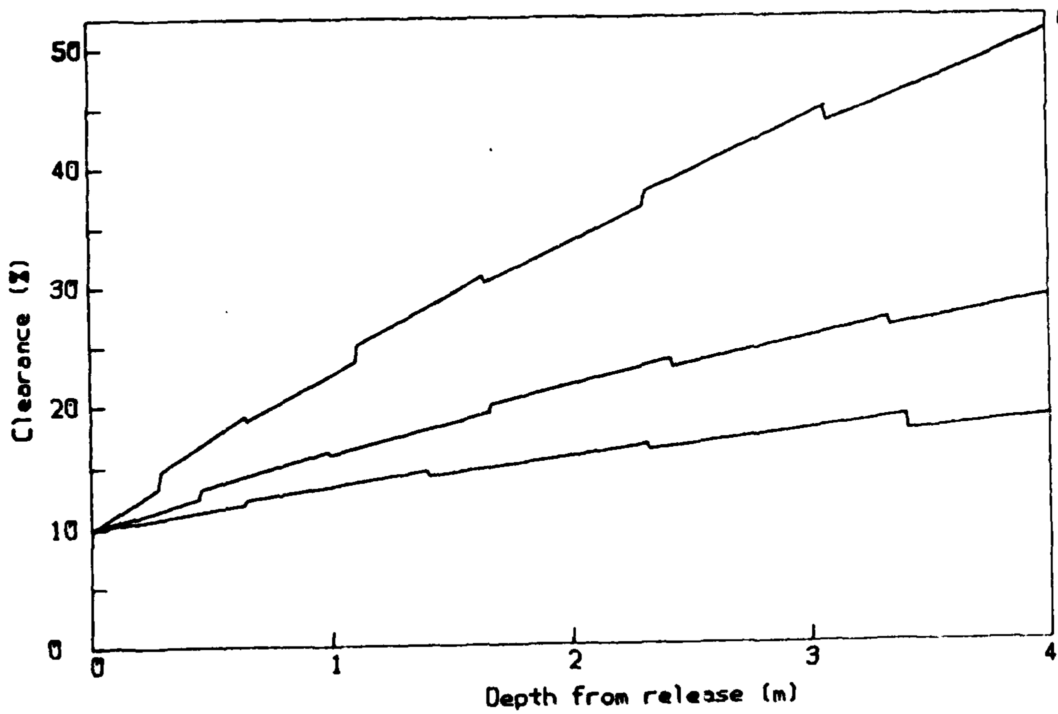

Drop diam (um) Init	Final	Path length (m)	Release rate (l/min)
60	129	182	1.83
80	135	145	3.90
100	143	118	6.89

Fog Dispersal Model Output
Fig. 4

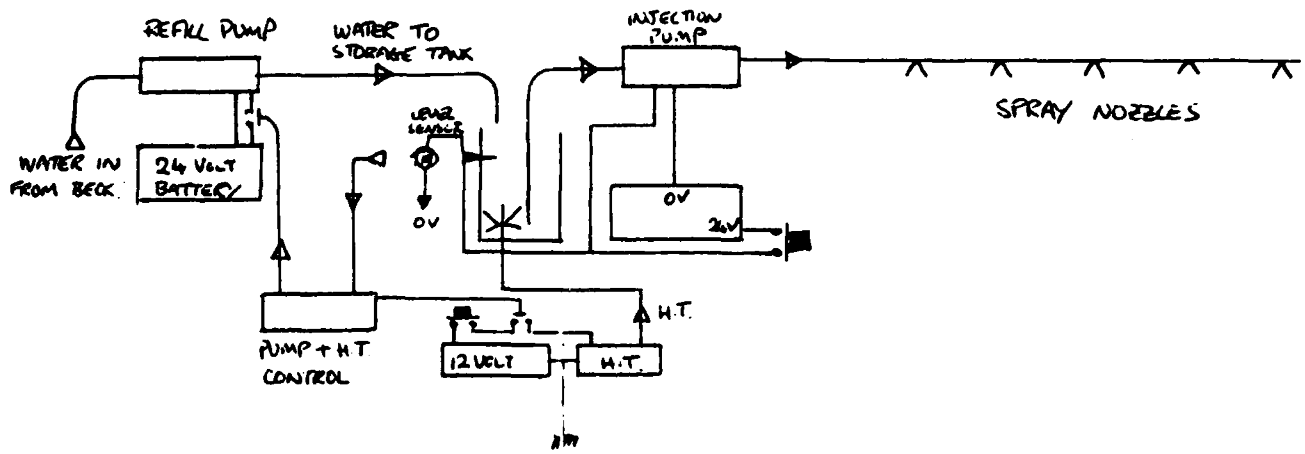

Release Site Schematic
Fig 5.

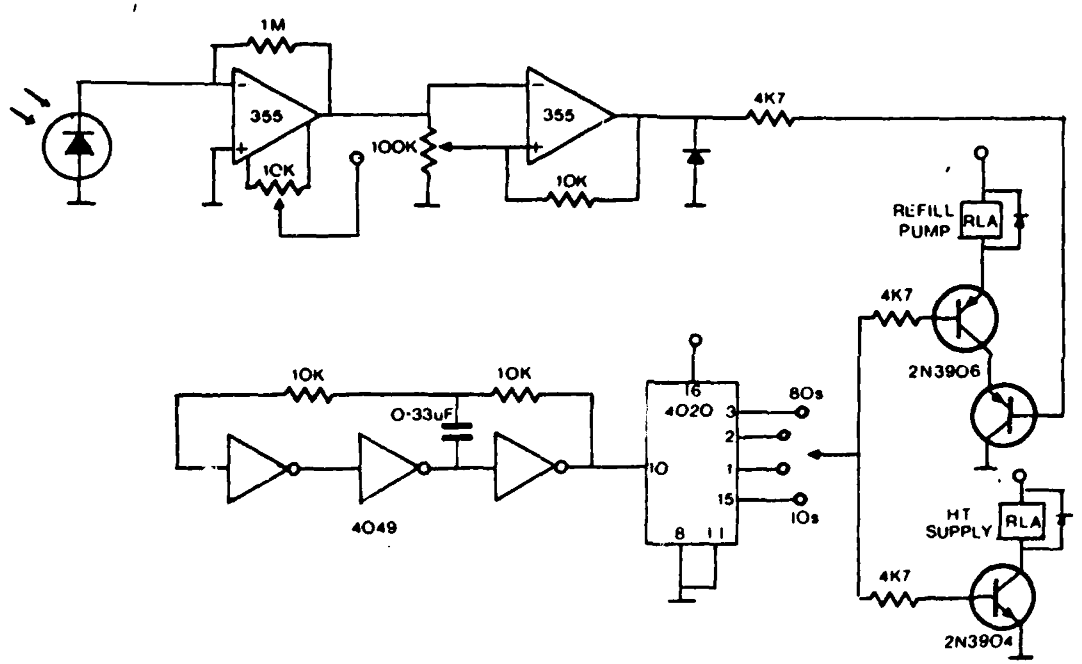

H. T. and Pump Control
Fig 6.

FIG. 7

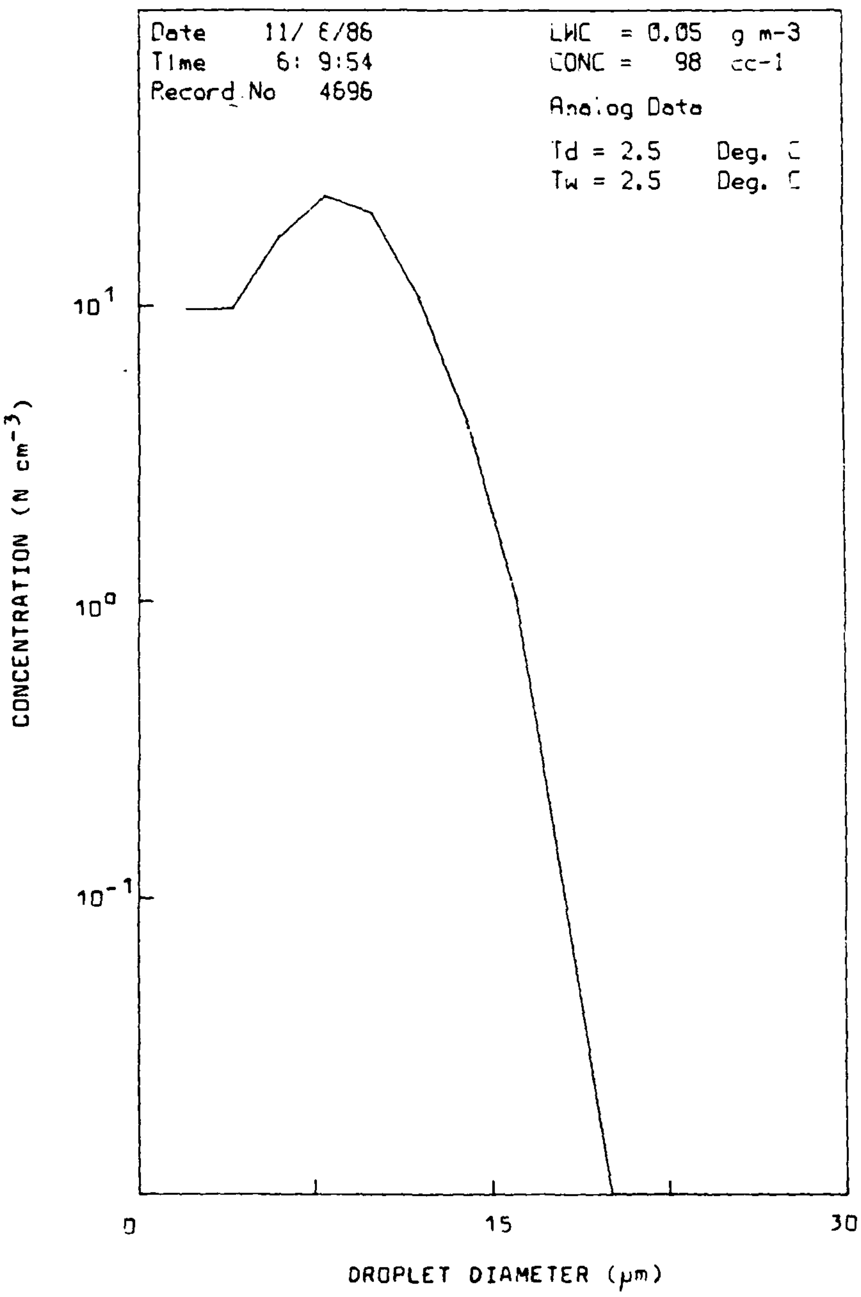

Date 11/ 6/86
Time 6: 9:54
Record No 4696
LWC = 0.05 g m-3
CONC = 98 cc-1
Analog Data
Td = 2.5 Deg. C
Tw = 2.5 Deg. C
10^1
10^0
10^-1
CONCENTRATION (N cm^-3)
0
15
30
DROPLET DIAMETER (μm)

FIG.8

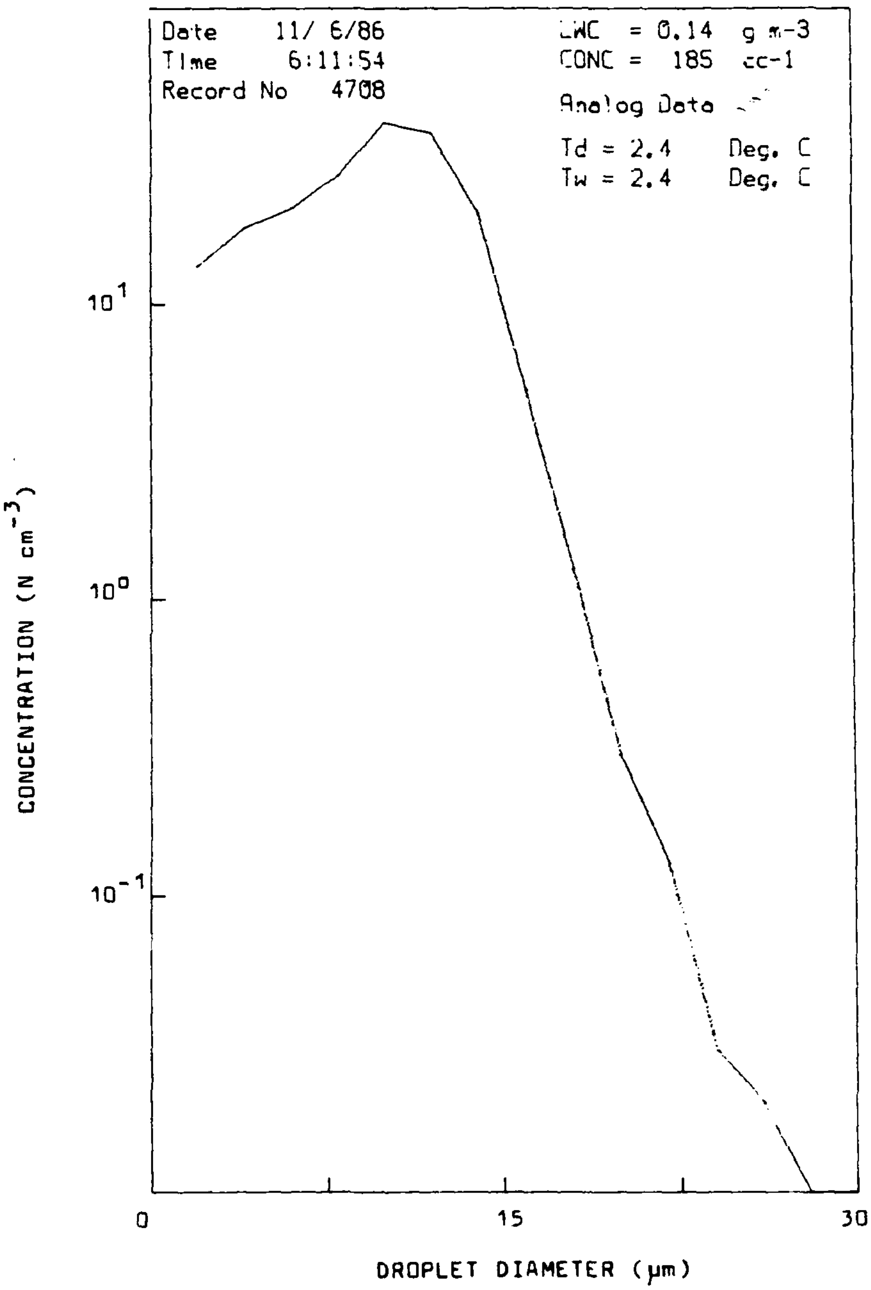

Date 11/ 6/86
Time 6:11:54
Record No 4708
LWC = 0.14 g m-3
CONC = 185 cc-1
Analog Data
Td = 2.4 Deg. C
Tw = 2.4 Deg. C
10^1
10^0
10^{-1}
CONCENTRATION (N cm^{-3})
0
15
30
DROPLET DIAMETER (μm)

FIG. 9

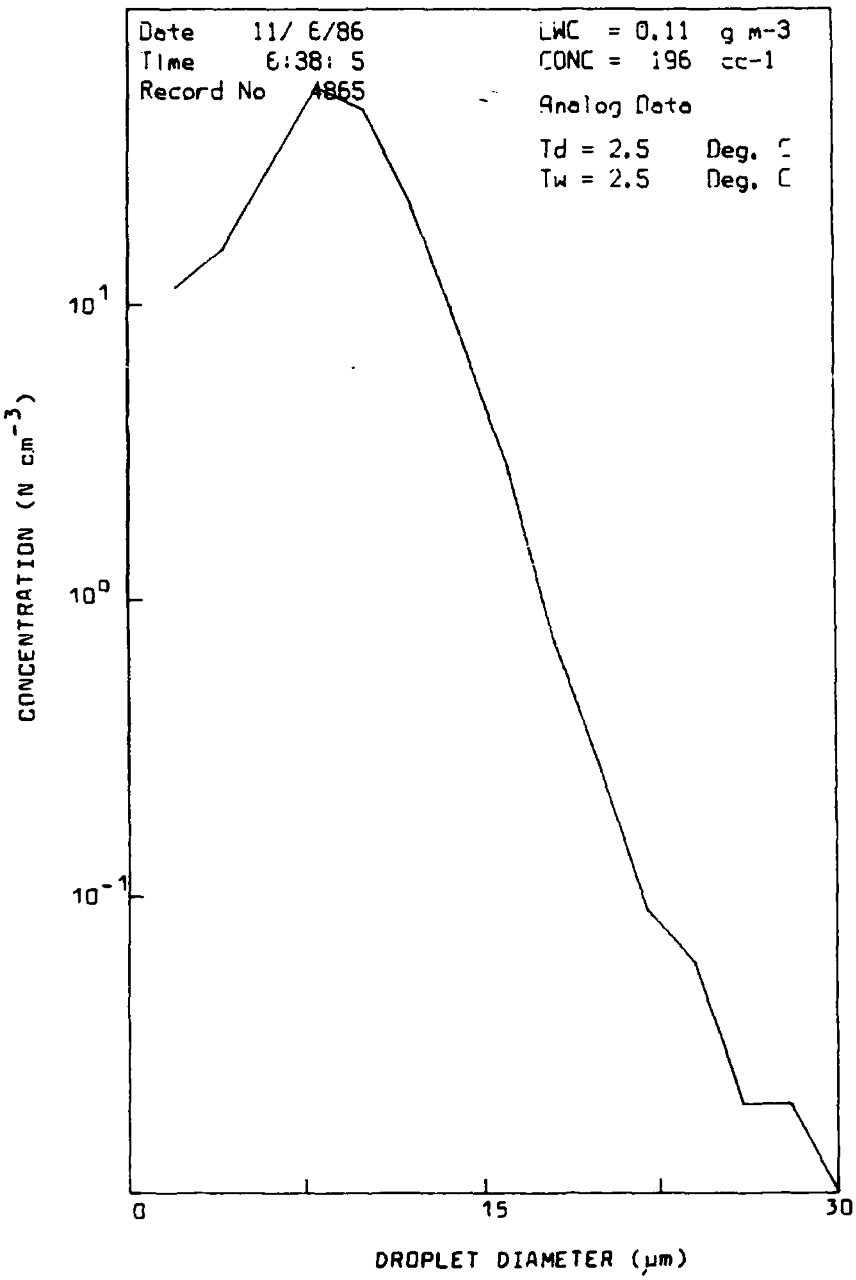
Date 11/ 6/86
Time 6:38: 5
Record No 4865
LWC = 0.11 g m-3
CONC = 196 cc-1
Analog Data
Td = 2.5 Deg. C
Tw = 2.5 Deg. C
CONCENTRATION (N cm-3)
10^1
10^0
10^-1
0
15
30
DROPLET DIAMETER (µm)

FIG. 10

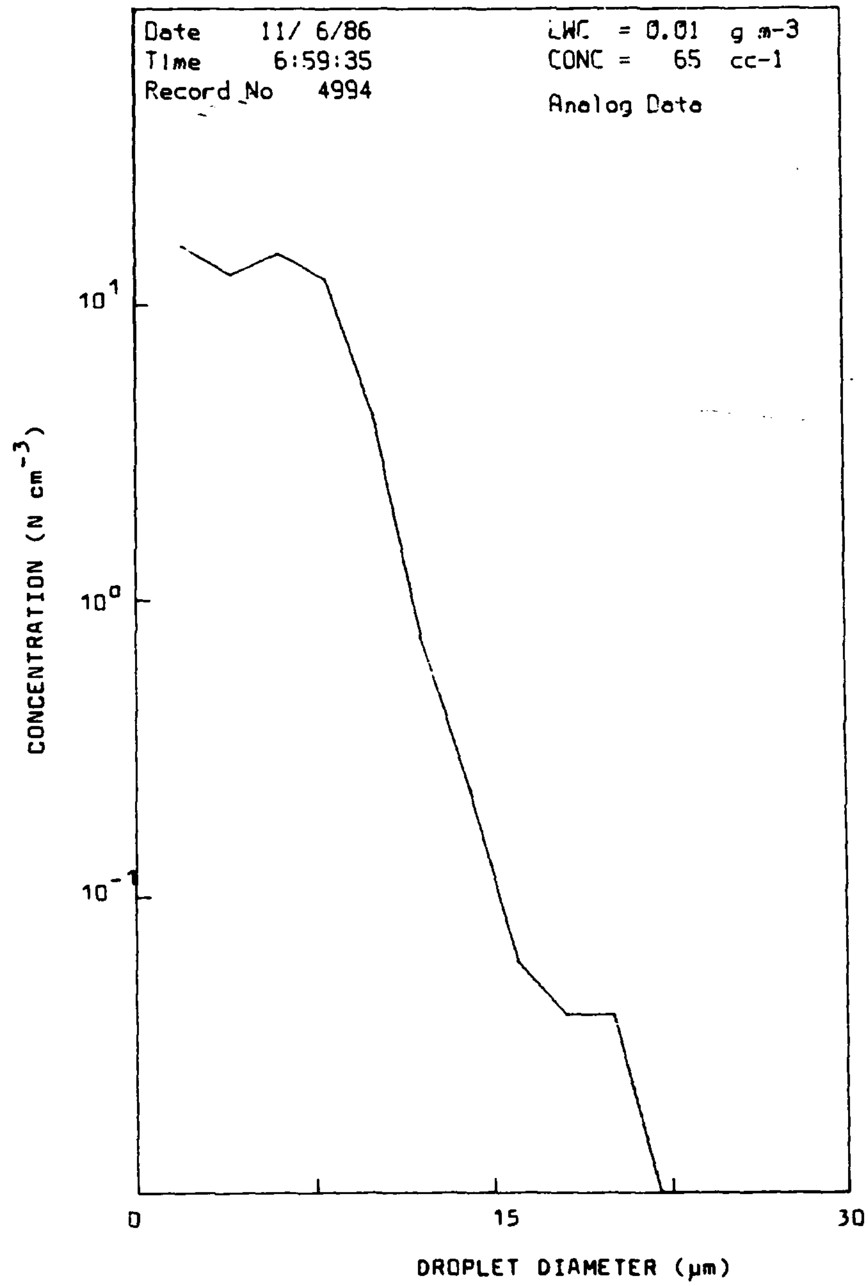

Date 11/ 6/86
Time 6:59:35
Record No 4994
LWC = 0.01 g m-3
CONC = 65 cc-1
Analog Data
CONCENTRATION (N cm^{-3})
10^1
10^0
10^{-1}
0
15
30
DROPLET DIAMETER (μm)

FIG. 11

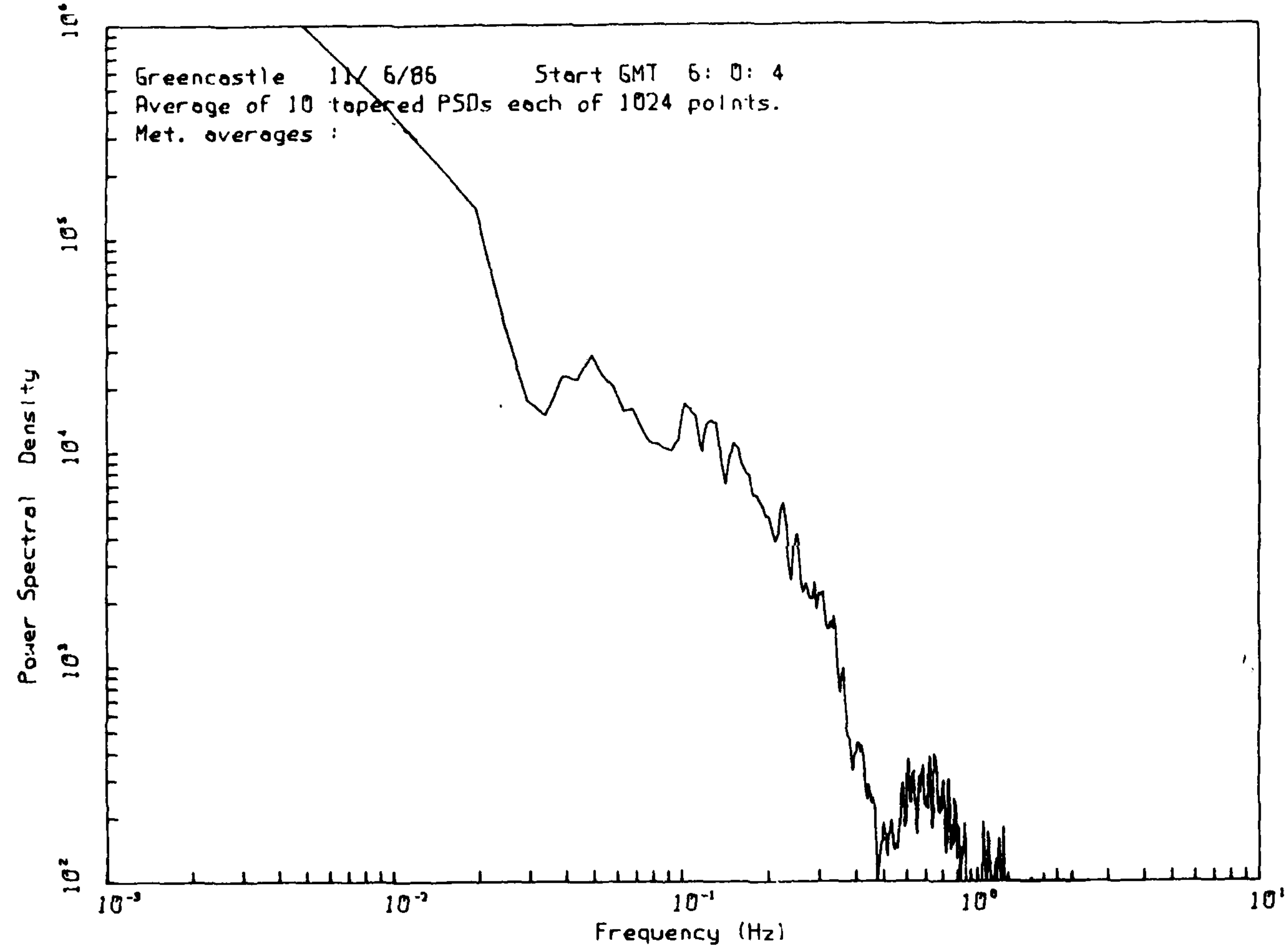
Greencastle 11/ 6/86 Start GMT 6: 0: 4
Average of 10 tapered PSDs each of 1024 points.
Met. averages :
Power Spectral Density
10^2
10^3
10^4
10^5
10^6
10^{-3}
10^{-2}
10^{-1}
10^0
10^1
Frequency (Hz)

FIG. 12

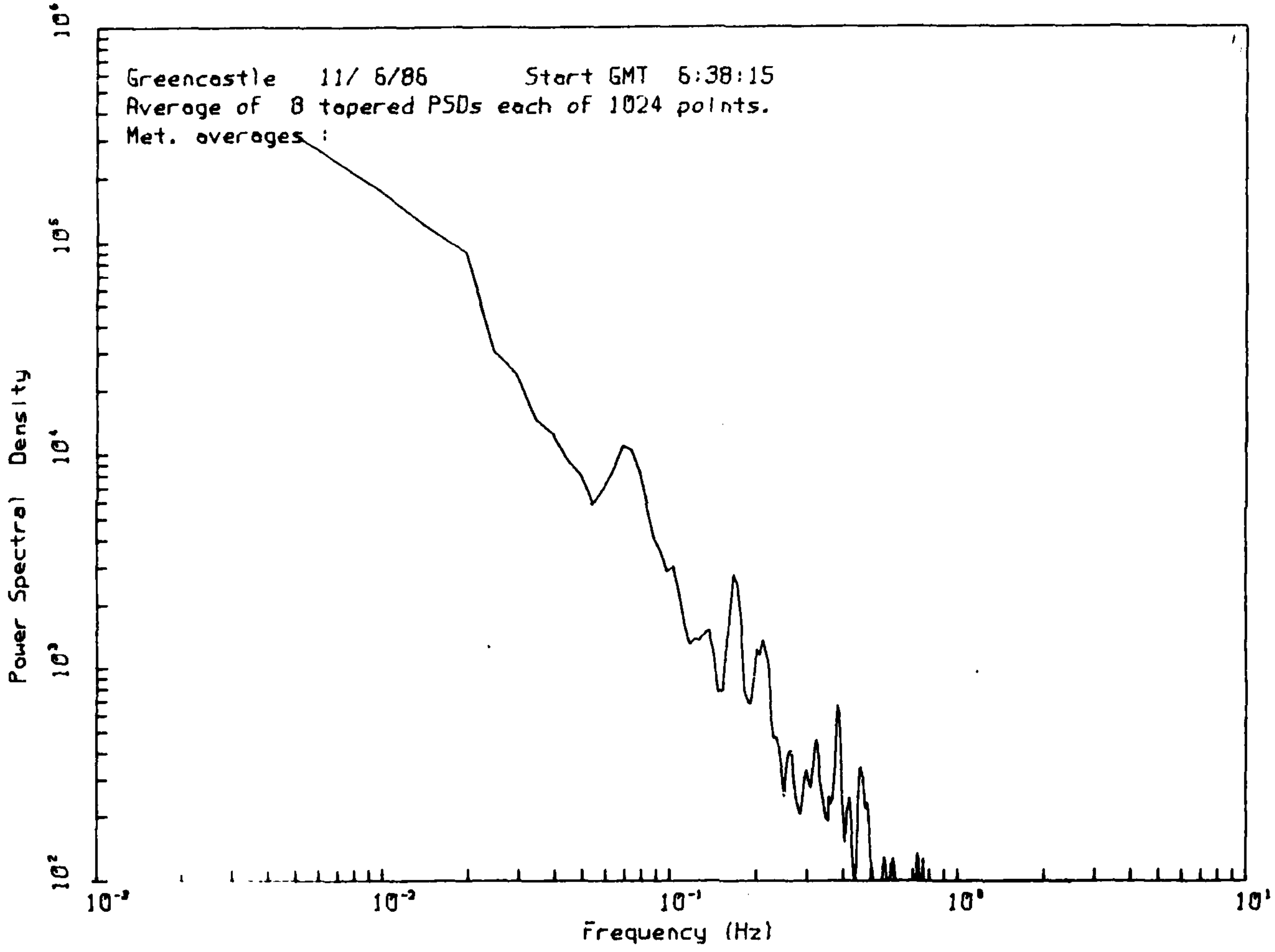

Greencastle 11/ 6/86 Start GMT 6:38:15
Average of 8 tapered PSDs each of 1024 points.
Met. averages :
Power Spectral Density
10²
10³
10⁴
10⁵
10⁶
10⁻³
10⁻²
10⁻¹
10⁰
10¹
Frequency (Hz)

FIG. 13

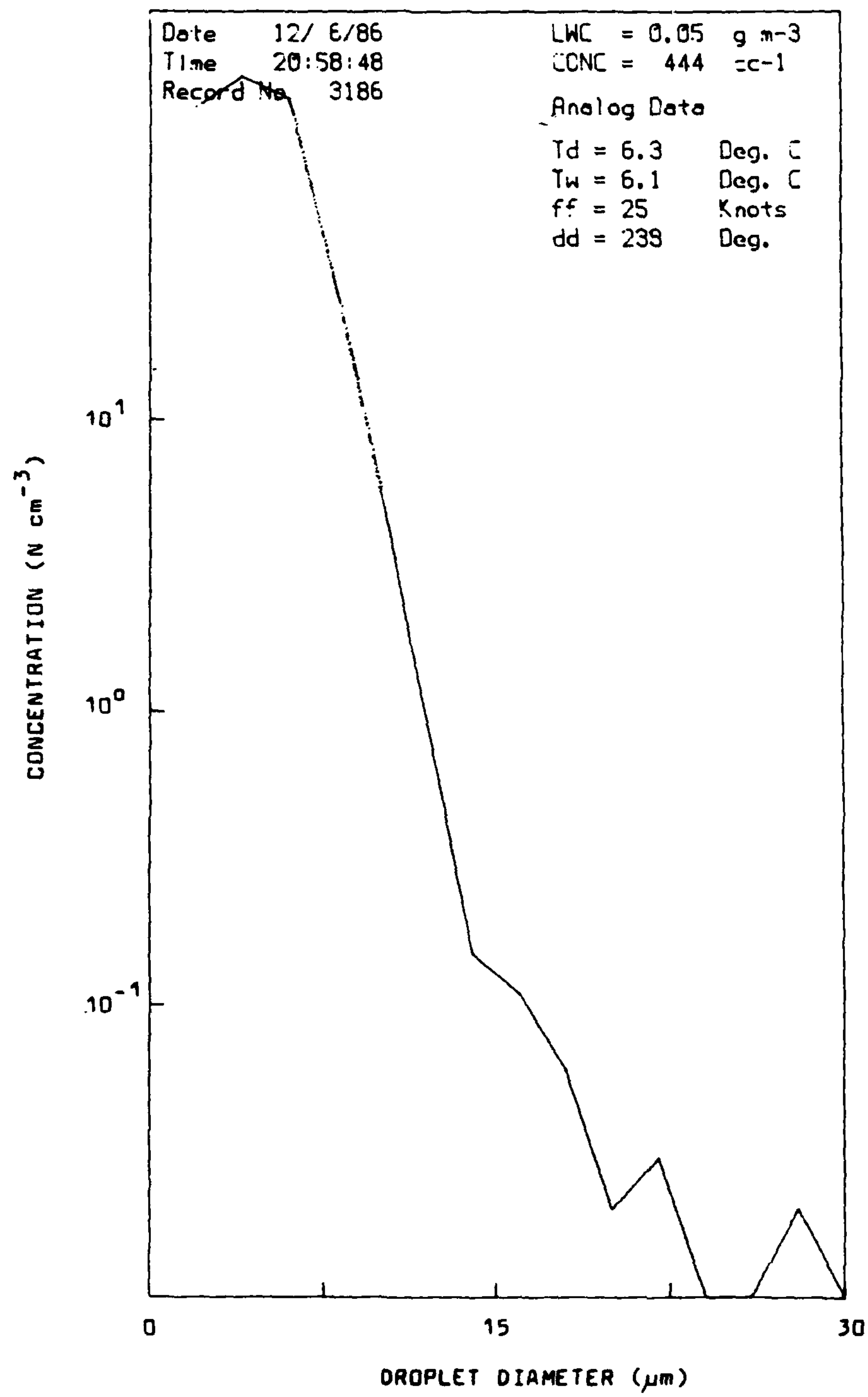

Date 12/ 6/86
Time 20:58:48
Record No. 3186
LWC = 0.05 g m-3
CONC = 444 cc-1
Analog Data
Td = 6.3 Deg. C
Tw = 6.1 Deg. C
ff = 25 Knots
dd = 238 Deg.
10^1
10^0
10^-1
CONCENTRATION (N cm^-3)
0
15
30
DROPLET DIAMETER (μm)

FIG. 14

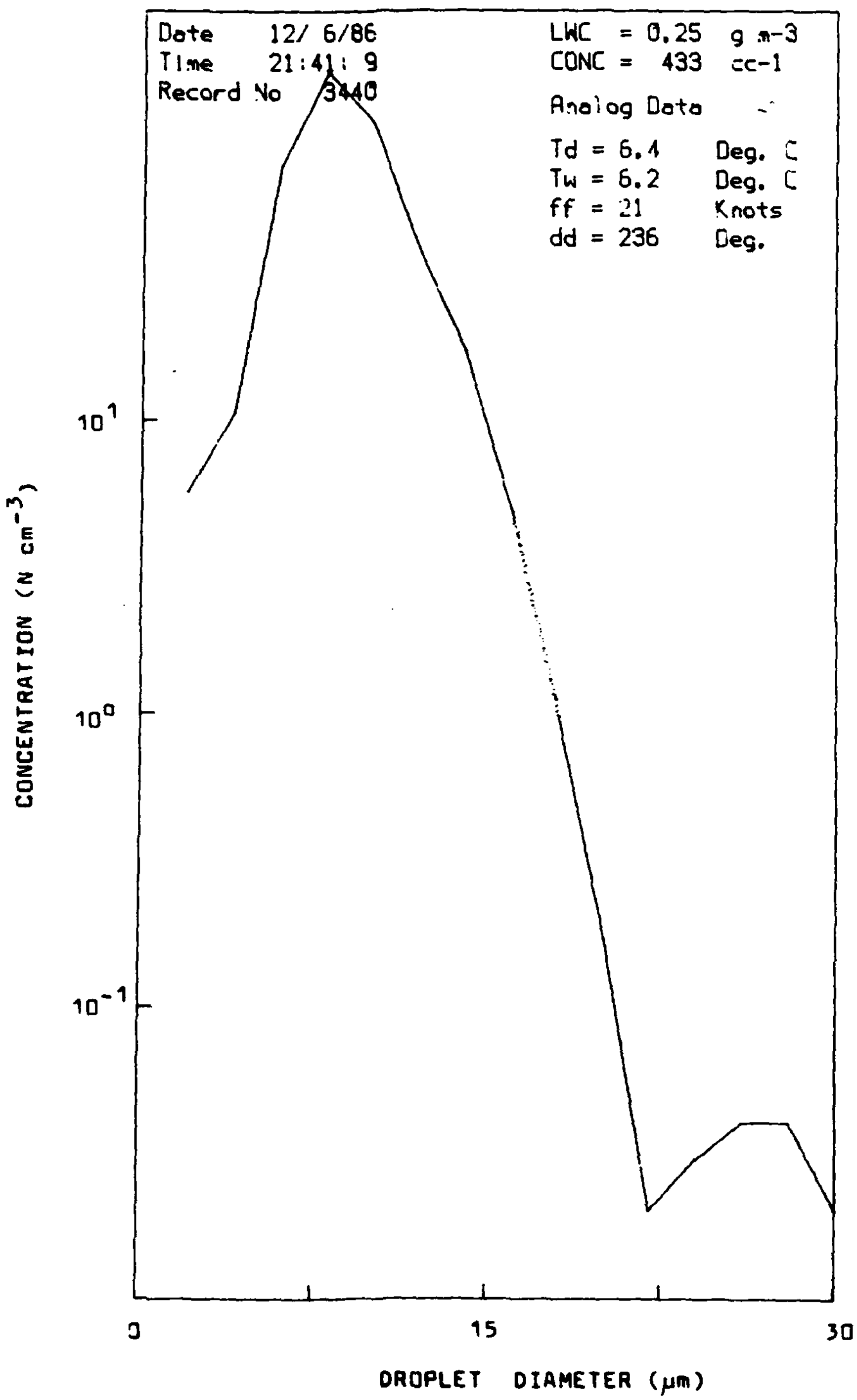

Date 12/ 6/86
Time 21:41: 9
Record No 3440
LWC = 0.25 g m-3
CONC = 433 cc-1
Analog Data
Td = 6.4 Deg. C
Tw = 6.2 Deg. C
ff = 21 Knots
dd = 236 Deg.
10^1
10^0
10^{-1}
CONCENTRATION (N cm^{-3})
0
15
30
DROPLET DIAMETER (μm)

FIG.15

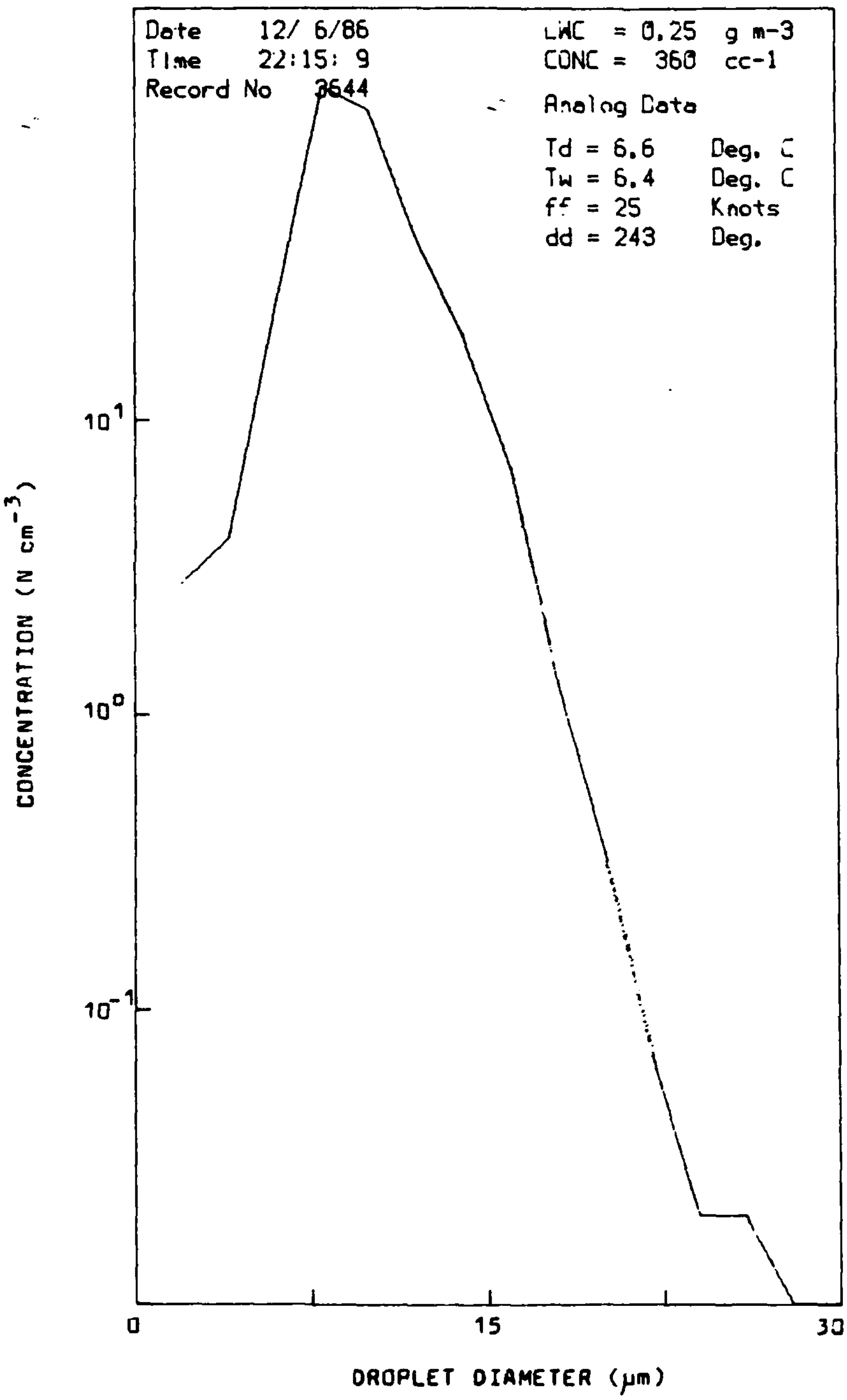
Date 12/ 6/86
Time 22:15: 9
Record No 3644
LWC = 0.25 g m-3
CONC = 360 cc-1
Analog Data
Td = 6.6 Deg. C
Tw = 6.4 Deg. C
ff = 25 Knots
dd = 243 Deg.
10^1
10^0
10^{-1}
CONCENTRATION (N cm^{-3})
0
15
30
DROPLET DIAMETER (μm)

FIG. 16

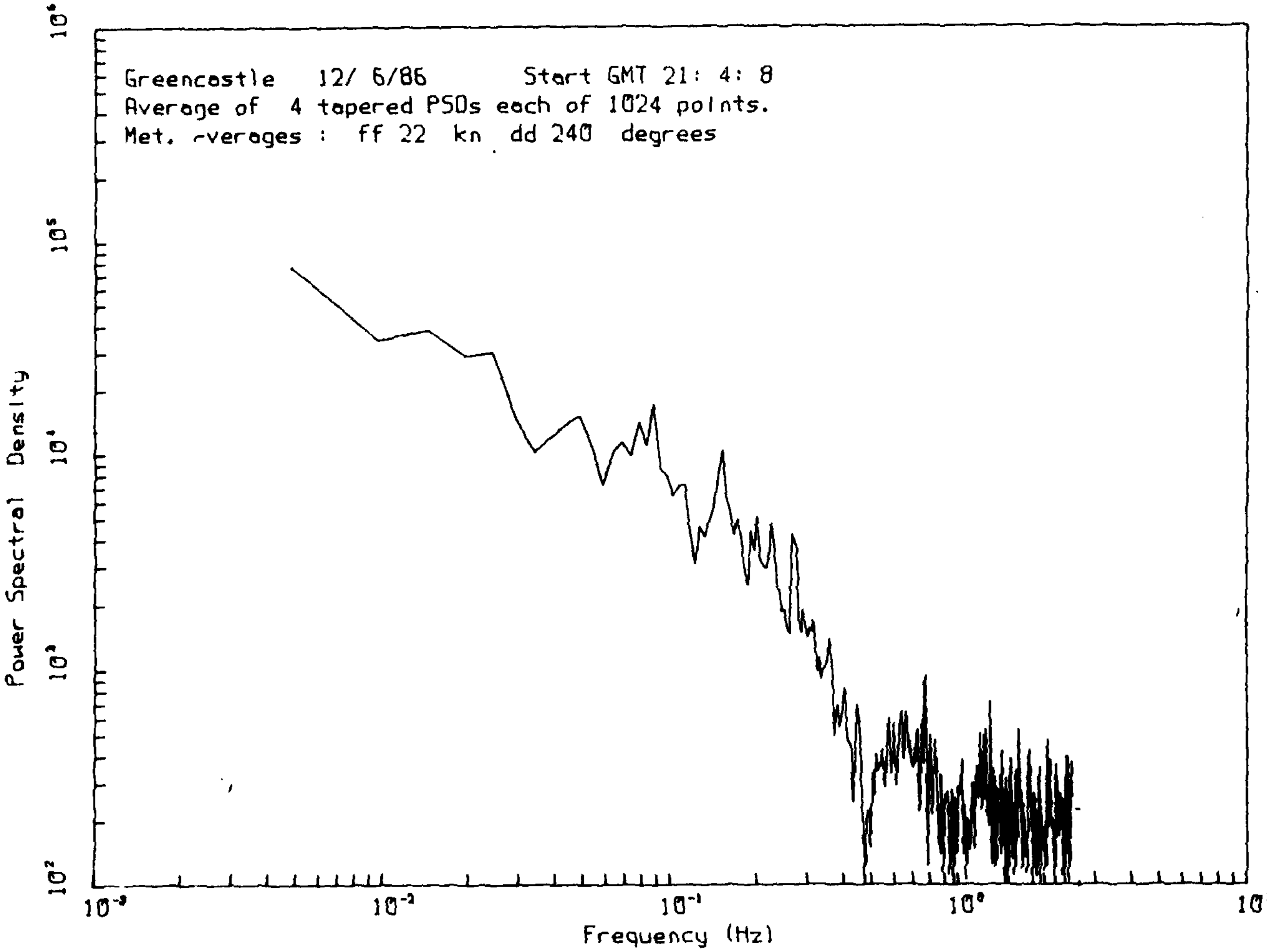
Greencastle 12/ 6/86 Start GMT 21: 4: 8
Average of 4 tapered PSDs each of 1024 points.
Met. averages : ff 22 kn dd 240 degrees
Power Spectral Density
Frequency (Hz)

FIG.17

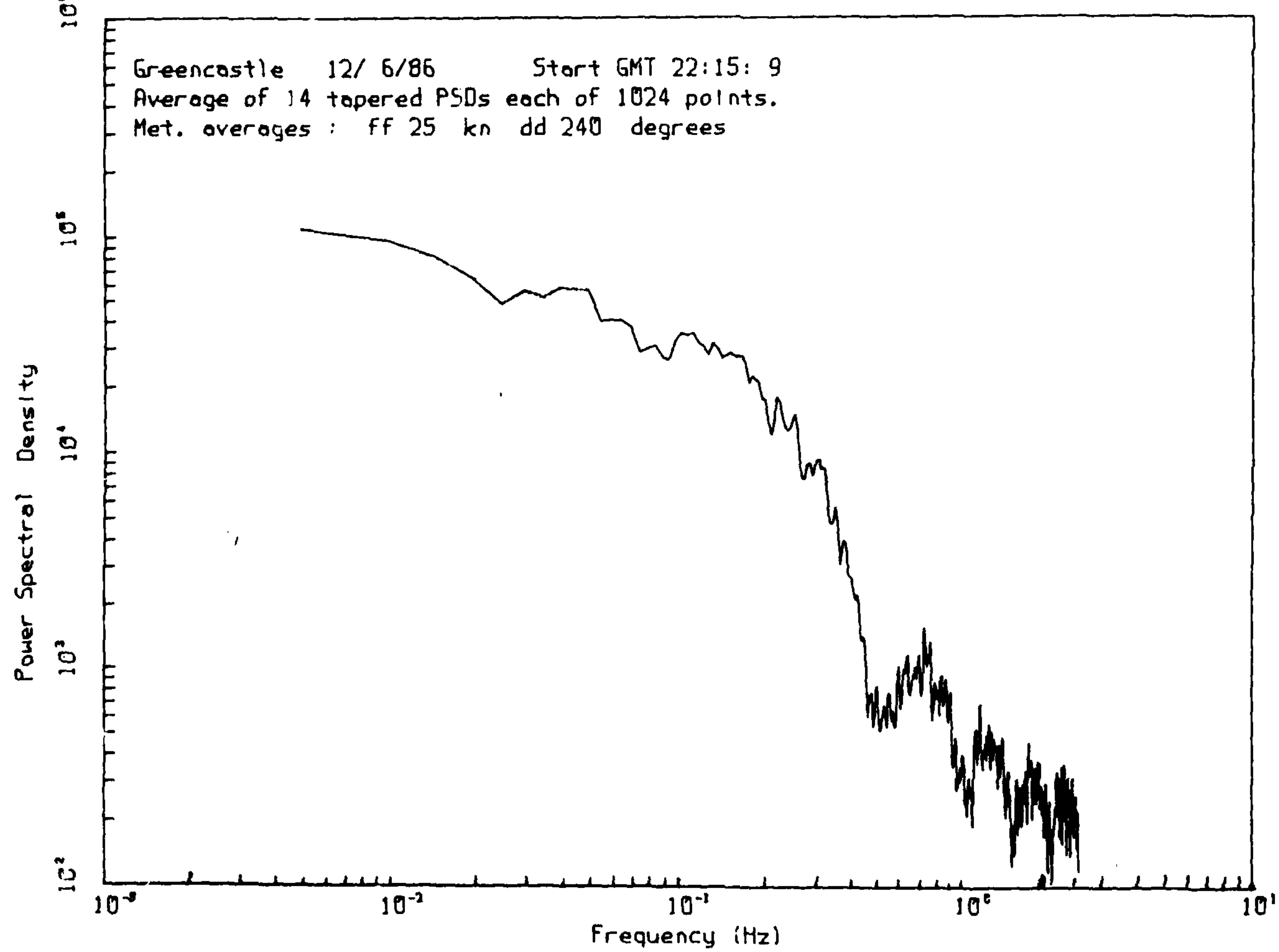
Greencastle 12/ 6/86 Start GMT 22:15: 9
Average of 14 tapered PSDs each of 1024 points.
Met. averages : ff 25 kn dd 240 degrees
Power Spectral Density
10^2
10^3
10^4
10^5
10^6
10^{-3}
10^{-2}
10^{-1}
10^0
10^1
Frequency (Hz)

END

DATE
FILMED

10-88